Models and Methodologies for Simulating Mobile Ad- Hoc Networks

Vinay Sridhara
Electrical Engineering
University of Delaware
Newark, DE, USA
vsridhar@udel.edu

Jonghyun Kim
Electrical Engineering
University of Delaware
Newark, DE, USA
kim@eecis.udel.edu

Stephan Bohacek
Electrical Engineering
University of Delaware
Newark, DE, USA
bohacek@udel.edu

Abstract

It is a truism that simulations of mobile ad hoc networks (MANETs) are not realistic. While the protocols are simulated reasonably realistically, the propagation of wireless transmissions and the mobility of nodes are not. Today, simulations typically model propagation with either the free-space model or a "two-ray" model that includes a ground reflection. Such models are valid only in open space where there are no hills and buildings. Since wireless signal at the frequencies used for MANETs is partly reflected off of buildings and is partly transmitted into the building, the presence of buildings greatly influences propagation. Consequently, these open-space propagation models are not accurate in outdoor urban areas. Indoors, the open-space models are not applicable. There has been little effort in developing realistic mobility models. In urban areas, the mobility of vehicles and pedestrians is greatly influenced by node interaction. For example, on a congested street or a sidewalk, nodes cannot travel at their desired speed. Furthermore, the location of streets, sidewalks, hallways, etc. restricts the position of nodes. Traffic lights also have a direct impact on the flow of nodes. In this paper, simulation of propagation and mobility for MANETs in urban areas is addressed. Techniques for simulation, models, model parameters, computational complexity, and accuracy are all examined. The techniques for propagation are validated against propagation measurements. Nearly all aspects of the mobility models and model parameters can be derived from urban planing and traffic engineering research. The simulation approaches discussed here are implemented in a suite of simulation tools that are available for download.

1 Introduction

Mobile ad hoc networks (MANETs) will likely be deployed in the future military operations. Furthermore, cities such as Philadelphia are planning to deploy ad hoc networks to provide wireless access to the entire 135 square mile city [36]. While the details have not been finalized yet, the initial plans for Philadelphia are that the network will include a large number of fixed wireless relays and perhaps mobile relays as well. Las Vegas has a pilot project already deployed for use by public safety organizations which is capable of supporting applications such as monitoring and controlling vehicular traffic for emergency response and remote situation assessment [6]. Over two hundred other local governments are considering similar projects. In such networks, end-hosts will certainly be mobile. Thus, large-scale deployment of multi-hop wireless ad hoc networks appears imminent.

It is well known that the variability of node-to-node communication is a major challenge facing MANETs. For example at one moment, high quality communication between two nodes may be possible while a short time later, communication between the nodes may not be possible. In the case of wide bandwidth communication, such drastic changes in link quality are typically the result of node mobility. For example, if a node moves around a corner of a building, then, since the signal is not easily able to penetrate through buildings; the communication between the two nodes may be severed. Thus, a combination of node mobility and complex propagation due to the environment results in rapid variability of communication links. However, while great strides have been made in protocols for MANETs, there has been very little effort devoted to understanding how to best simulate MANETs, specifically, how to best simulate the node mobility and signal propagation. This lack of effort contrasts the simulation of wired networks where there has been extensive work focused on simulation issues such as background traffic and topology (e.g., [11], [25], [13], [24]). This paper focuses on the techniques for simulating propagation and mobility of MANETs in urban environments and related issues. The simulation techniques presented here have been incorporated into a suite of simu-

lation tools *"UDelModels"* that are available for download.

At the frequencies used in today's wide band communication, wireless signals may undergo reflections off of buildings, reflections off of the ground, transmissions through walls, and diffractions over and around buildings. Thus, a wireless communication extends far beyond what line-of-sight (LOS) communication will offer. Indeed, our simulations show that majority of a node's neighbors (i.e., the nodes with which a node can communicate) are not within LOS. Similarly, Table 6 provides an example where the coverage area of a single transmissions increases by 450% when reflection, transmission, and diffraction are included. As will be discussed in Section 5.3, the variation of the signal strength under LOS propagation is significantly different from the variation of the signal strength in reality. Goals of realistic propagation simulation include simulating realistic coverage and realistic variation of the signal strength.

There has been extensive work on modeling and understanding realistic topologies that arise in wired networks (e.g., [13], [24]). In MANETs, the study of topology is complicated by the dependence on the propagation characteristics of the environment and location of the nodes. Propagation and the location of nodes is not random, but is dominated by structure. For example, streets, especially well traveled, wide, and straight, have high node density and excellent propagation properties. Thus, nodes on a major street will have a large number of other nodes within communication range. However, these nodes will not be able to directly communicate with nodes on parallel streets since such communication requires transmissions through buildings or over them; something that is difficult if the buildings are large. Hence, the topology in an urban environment with large buildings will consist of well-connected nodes along the streets. Nodes near intersections will provide connectivity between two streets. Hence, the topology of outdoor nodes looks like a street map of the city. Within buildings, nodes have a smaller propagation range. Thus, the local topology of indoors and outdoors is very different. Realistic topologies can be simulated only if the propagation and mobility simulations are realistic.

Current approaches to mobility will be discussed in Section 6. There is little doubt that these mobility models are not realistic. To some extent, since open-space (i.e., free-space and two-ray) propagation models that neglect the impact of objects have been used in the past, there has been little reason to use mobility models where nodes avoid or interact with objects. However, when propagation in urban environments is considered, mobility must also be addressed. Specifically, the mobility model must take into account the structure of the urban environment such as streets, sidewalks and buildings.

One of the reasons that mobility models must not be overly simplified is that in reality pedestrians and vehicles tend to move in clusters [38], [46]. That is, the locations of nodes are correlated. Furthermore, there is a well-studied relationship between node density and node speed (e.g., recall the "two-second rule" that specifies the safe driving distance between cars). Since the spatial distribution of nodes has an important impact on the behavior of MANET protocols, mobility models must be realistic.

In summary, the objectives of the simulation approach discussed here is to provide realistic simulation of mobility and propagation. Specifically, for mobility, the goal is to provide realistic

– node distribution,
– node clustering (i.e., correlation in node location),
– trips including trip lengths, paths, and generation rates,
– and node speeds.

For propagation simulation, the goal is to provide realistic

– propagation range,
– signal strength,
– and spatial variation of the link quality.

Together, the mobility and propagation simulators provide realistic

– topologies,
– and variations of topologies.

The mobility simulation objectives can be achieved by employing models and model parameters that have been developed and verified by the urban planning and traffic engineering research communities. The propagation simulation objectives can be achieved by verifying and by comparing the propagation model to observations. If the mobility and propagation are realistic, then the topology and the dynamics of the topology should be realistic. However, this can only be verified when MANETs are deployed.

It is important to note that the objective is realistic simulation, not accurate simulation. By this we mean that the simulation should provide mobility and propagation similar to what *could* occur in an urban environment, not necessarily what *would* occur in a particular urban environment. As will be discussed, accurate prediction requires substantial knowledge of the modeled urban environment. For example, accurate prediction requires precise knowledge of location and dimensions of buildings and other large to moderate sized structures, as well as knowledge of the building materials used and the layout of building interiors. Furthermore, accurate mobility simulation requires knowledge of details such as the types of establishments within each building (e.g., restaurant, office, shopping, etc.) and origin-destination flow matrices for vehicle traffic. Realistic simulation, on the other hand, merely needs realistic dimensions and locations of buildings, building materials, layout of buildings interiors, and realistic trip generation for vehicles and pedestrians.

The motivation for realistic simulation rather than accu-

rate prediction is to reduce the complexity of simulation. There are two types of complexity that are relevant here, computational complexity and usage complexity. The latter refers to the difficulty in defining the simulated environment. This paper provides models and parameter values, and discusses tools to develop simulated environment that satisfy the goal of realistic simulation. If the goal is realistic simulation then the complexity of use is reduced. Computational complexity is treated in detail in Section 5.1.

Propagation, vehicle mobility, and pedestrian mobility modeling are all active areas in research. Addressing all these issues is beyond the scope of this paper. Instead the focus of this paper is on topics that are most critical.

The remainder of the paper proceeds as follows. In the next section, previous work related to simulation of propagation and mobility for MANETs is discussed. Section 3 provides a short overview of the steps involved in simulating MANETs. Section 4 discusses different approaches to defining city maps that can be used for mobility and propagation simulation. Section 5 discusses characteristics and simulations of propagation. Section 5.1 examines the computational complexity of propagation simulation for MANETs. Section 5.2 discusses the impact of reflections and diffractions in propagation in urban areas. Section 5.3 provides validation of the propagation models. Section 6 discusses mobility models for realistic MANET simulation. This discussion is broken down into the following sections. Section 6.1 the dynamics of nodes and section 6.3 discusses trip generation. Section 6.4 provides some validation of the pedestrian mobility model. Section 7 provides concluding remarks.

2 Related work

Currently, Open-space propagation (i.e., free-space and the two-ray model) is the most popular propagation model for MANETs research. For example, ns-2 [29], [30] only supports open-space propagation models. On the other hand, QualNet [42] supports open-space propagation as well as stochastic propagation models such as Rayleigh, Rician and Lognormal fading. QualNet also supports path loss trace files. Furthermore OPNET [33] supports open-space propagation models as well as an enhanced open-space model that accounts for hills, foliage and atmospheric affects.

While less popular, stochastic models such as Rayleigh, Rician and Lognormal fading [39] have been used by several investigators. In order to include correlations, Markov model based stochastic models have been suggested [23], [43] While such propagation modeling is useful to compare physical layer techniques, they have limited use in MANETs. The drawback of stochastic propagation models is that they fail to model the propagation structure found in urban areas. As mentioned earlier, due to the difficulty of propagating through buildings and the ease of propagating down the streets, the topology of the outdoor nodes in a MANET resembles the street map of the city. Also, propagation indoors exhibits structure due to the floors and hallways.

In [18] and [17] obstacles were included in the simulated environment and propagation was limited to line-of-sight. In [17] the obstacles were randomly placed buildings. As will be shown most of the communication in an urban area is not line-of-sight. Since streets play an important role in MANET topology, the random placement of buildings will result in non-realistic topologies.

There has been limited work that includes accurate propagation modeling along with MANET simulation. For example, [8] suggests using ray tracing indoors to enhance ns-2's propagation model.

Instead of simulation, there has been some effort in developing desktop test-beds [21]. Such test-beds augment protocol simulation with live wireless transmissions over a small wireless network. A significant drawback of such an approach is that it is not able to realistically model the multipath reflection, transmissions, and diffractions that occur in a complicated propagation environment.

There are several commercial packages that can be used to predict coverage of a single or a small number of mobile phone base stations or wireless access points (examples include [48] and [47]). While many of the propagation techniques used by these tools are employed by a MANET propagation simulation (e.g., [41]), these tools have limited applicability to MANET simulation, due to different goals (realistic vs. prediction). Specifically (as discussed earlier) the goal of accurate prediction increases the computational complexity as well as the complexity of use. Most tools focus on outdoor coverage for mobile phones, or indoor coverage for wireless base stations; they neglect mixed indoor/outdoor simulation. These tools do not produce a propagation matrix as required for simulation.

There are several mobility models used for MANET simulation. The most popular is the random waypoint model [19] where a node picks a next destination at random. The node travels in a straight line to the destination at a randomly selected speed (often uniformly distributed between 1m/s and 20m/s). Upon arriving at the location, the node waits for a random amount of time before selecting the next location. There are many variations in such random (see [5] for details and references) mobility models. In [18] several scenario based mobility models were considered. However, as mentioned in [18], these mobility models are not meant to be realistic. In [2], the Manhattan mobility model is introduced where nodes are restricted to a grid, resembling the street map of Manhattan. This model does not include any realistic node mobility dynamics (e.g., node interaction,

traffic lights) or realistic trip generation. In [34], mobility patterns from multi-user games were used, but did not verify that the mobility of characters in games resemble the mobility of pedestrians or vehicles.

3 MANET simulation overview

There are several stages to MANET simulation. The first step is to define the simulated city map. This step is discussed in Section 4. The second step is to determine the propagation matrix for the city. The propagation matrix includes channel characteristics such as path loss, delay spread and angle of arrival for each source-destination in the city. This step is discussed in Section 5 Next, the city map is used to generate one or more mobility trace files. This step is discussed in Section 6. From the mobility trace file and the propagation matrix, the propagation trace file is computed; the propagation trace file provides the propagation statistics between all pairs of nodes at every moment. The propagation trace file can then be used by the protocol simulator.

4 City maps

In order to model MANETs over urban areas, it is necessary to have a model of the urban area. There are several ways that maps suitable for MANET simulation can be developed. First, a random city can be built as was done in [17]. In this case buildings are placed at random and a Voronoi diagram is used to construct sidewalks between the buildings. One drawback of such an approach is that important aspects of cities such as long thoroughfares and big intersections are neglected. It is well known that streets play an important role in mobile phone communication and it has been shown that streets play an important role in urban MANET connectivity [4].

A more realistic way to generate cities is to utilize the detailed GIS datasets [12]. These datasets include 3-dimensional building map information that provides enough detail for realistic simulation. There is an abundant number of such datasets. For example, there are GIS datasets for most, if not all, American cites. Our map building suite of tools converts GIS datasets into format suitable for a specialized graphical editor. The graphical editor is used to ”touch-up” the GIS map (e.g., remove spurious buildings, add roads, sidewalks, traffic lights, and fixed base stations). The graphical editor is also used to define locations where vehicles enter and exit the modeled area.

A third way to generate city maps is to develop a map directly in the editor. For example, idealized grid city could be generated within the editor. And finally, there has been some work on generating random, yet realistic cities [35]. Often, random cities produce GIS datasets, and hence are easily used for propagation and mobility simulation. These realistic random cities are often generated to meet certain aesthetic requirements. It is unclear if these random cities would span a relevant range of mobility and propagation. In the same way that random wired network topology generation required substantial effort before relevant topologies were developed, random city generation for MANET simulation will also take considerable effort.

While GIS datasets have details of building heights and position, they typically do not provide any details about the interiors of the building. In lieu of actual interiors, they must be automatically generated. Our suite of tools assumes that all buildings are office buildings with offices that are 3.5 meters wide and 3/8 of the building depth deep and the width of hallways is 1/4 of the depth of the building. The hallway runs in the center of the building and stairs are on each end of the building. Incorporating automatic generation of heterogeneous building interiors will be left for future work.

5 Propagation modeling

The main factors that affect the probability of a packet error are signal strength, delay spread, Doppler spread, and noise, which include interference. Of these, current simulators only consider signal strength and interference. Delay spread accounts to the fact that a single transmission might result in several delayed signals arriving at the receiver. Each of these signals follows a different path and hence arrive at a different time and with different amplitude. If the delay between these signals is sufficiently large, they can increase the probability of transmission errors. Similarly Doppler spread also contributes to increased packet error rate. Doppler spread results when the transmitter, receiver, or an object that the signal reflects off of is moving.

There has been little work that relates delay spread and Doppler spread to packet error probability. The reason for this might be the fact that the signal strength plays a more significant role in the packet error probability [39]. If signal strength can be computed, it is straightforward to compute delay spread (our implementation determines delay spread) but further investigations are necessary to arrive at a relationship between delay spread and packet error probability. The section focuses on estimating the signal strength[1] in urban environments

The signal strength at the receiver is given by $P_{\text{Received}} = P_{\text{transmitted}} \times C \times \textit{Path Loss}$, where C is a constant that depends on the antennas and the frequency, and is often on the order of -30dB to -40dB. Assuming that C is known, and if the transmitted power is known, then knowing the path

[1] Note that signal strength is also used to determine interference.

loss is equivalent to knowing the signal strength. Thus, the terms path loss and received signal strength are used interchangeable.

A large volume of research has shown that at the distances and frequencies considered here, the propagation of electromagnetic waves can be modeled as rays (see [40] and reference therein). These rays reflect off of the ground and walls, are transmitted through walls, and diffract around corners. While traveling through free-space, the ray's signal strength decays like $1/d^2$ where d is the distance. When the ray makes a reflection, transmission, or diffraction, it experiences an additional decrease in signal strength and a change in phase. Thus, the path loss for a particular ray is given by

$$\text{Path loss} = 1/d^2 \times Attenuation, \tag{1}$$

where $Attenuation$ is a complex number that depends on the details of each reflection, transmission, and diffraction. The received signal strength can be determined by finding all the rays that hit the receiver and determining the length and the attenuation experienced by each ray. Determining the received signal strength at a particular frequency requires the addition of signal strength provided by each ray. For wide band communication, the signal strength is the average power of the signal averaged over the bandwidth. For example, in 802.11b, the signal is averaged over the 22MHz wide channel that is centered at 2.414GHz. Averaging is not necessary when narrow band communication is used.

The attenuation and change in phase due to a reflection or transmission depends on the frequency and polarization of the signal[2], the angle of incidence, and the type and the thickness of the material that the signal is reflecting off of or transmitting through. If the material is known and is homogeneous, the loss and change in phase can be found in a straightforward manner (e.g., see [20]). Figure 1 illustrates how attenuation of the signal depends on the material and the angle of incidence. Figure 1 shows that the difference between glass and concrete is less than 10dB. Other materials such as brick result in similar variations in loss, while materials such as wood have a significantly different behavior. Since it is not possible to know the material used in the construction of all buildings, the attenuation from reflection and transmission is difficult to be exactly determined. However, since the goal is for the simulations to merely be realistic, path loss can be obtained by assuming that common building materials are used (e.g., concrete, brick, and glass, which all have similar propagation characteristics).

Besides reflection and transmission, diffraction plays an important role in propagation. Diffraction allows wireless transmissions around the corners and over the buildings. Whether a signal is more easily diffracted over the building

[2]It is typical to assume vertical polarization.

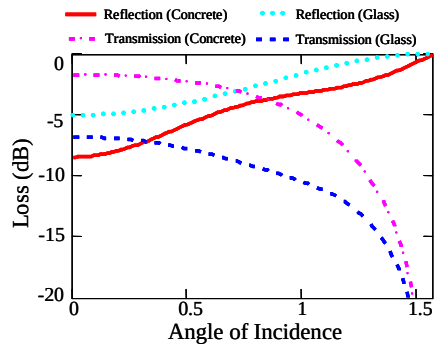

Figure 1. Loss due to Reflection and Transmission. The plot assumes that the concrete is 20cm thick and the glass is 2cm thick.

or transmitted through the building depends on the size and height of the building. Thus, both transmission and diffraction must be modeled. The Uniform Geometrical Theory of Diffraction has been shown to provide a realistic model for diffraction.[26].

Once the map, bandwidth, and building materials have been defined, propagation can be determined. However, extreme care must be taken to reduce the computation. Assuming that all walls are vertical significantly decreases computational. Specifically, the 3-D ray tracing problem reduces to a 2-D ray tracing problem that finds vertical plane paths. The 2-D ray tracing problem is illustrated in the right-hand plot in Figure 2, where two vertical plane paths are shown. Once the vertical plane paths are found, the 3-D ray paths restricted to the vertical plane paths can be computed easily. The left-hand figure in Figure 2 shows the paths of a ray in the vertical plane. One vertical plane path has three ray paths, (a1) one that diffracts over a building, (b1) one that reflects off of the ground and passes through a building, and (c1) the one that passes straight through a building. The other vertical plane path has two ray paths, (a2) one reflecting off of the wall of a neighboring building and (b2) one reflecting off of the wall of neighboring building and undergoing a ground reflection. In one vertical plane path there are potentially many ray paths that include repeated reflection off of the ground, transmission through buildings, and diffractions over buildings. In our simulator, we include three types of ray paths, direct paths (line of sight or transmissions through buildings), ground reflected paths, and paths that diffract over buildings without being transmitted through the buildings. For paths that diffract over buildings, if the transmitter or receiver is indoors, then the ray path passes through the building where the transmitter and/or receiver is, but must pass over all other buildings intersected by the vertical plane path. Such ray paths

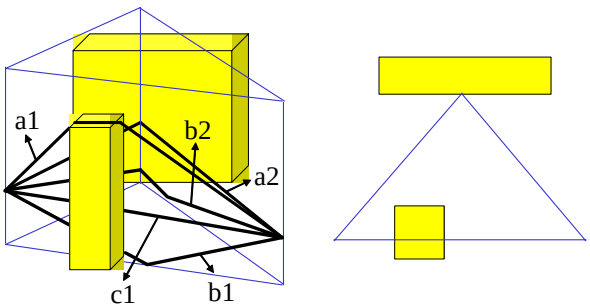

Figure 2. Left: Two vertical plane paths and 5 ray paths. Right: a top-view of the scene on the left.

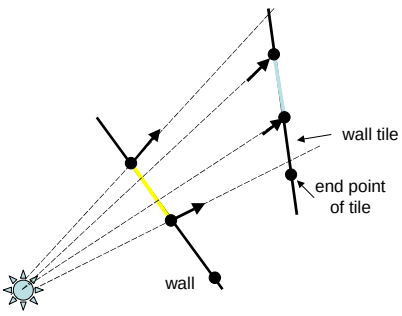

Figure 3. Beam Tracing. Suppose that the (yellow) tile on the lower left has been determined to be hit by a beam. In particular, this beam hits the end points such that the reflected rays are as shown. From these rays, the virtual source, shown in the lower left, is found. The angle at which the beam hits the end points of the (blue) tile in the upper right is found as shown. This tile generates a reflected and transmitted beam and the process continues.

do not have a significant impact on the computed path loss since transmissions through buildings and diffractions over buildings greatly reduce the signal strength.

A straightforward implementation of even 2-D ray-tracing is not computationally efficient. Instead, a technique that is more appropriately called beam tracing can be performed. Like ray tracing, the goal of beam tracing is to determine the paths from the transmitter to receiver. Beam tracing begins with the source broadcasting the signal in all directions (assuming an omnidirectional antenna). This transmission is not modeled as a large number of rays, but as a small number of beams. When a beam intersects a building, two beams are generated, one is reflected off of the building and one is transmitted into the building. If only a part of the beam intersects the building, the beam is split into three with one part of the beam continuing to the next wall (if it exists) and the other part of the beam generating two beams, a reflected beam and a transmitted beam. Finally, if the receiver is found to be included within the span of a beam, the ray from transmitter to receiver can be computed easily.

The beam tracing computation can be further simplified by dividing the 2-D space into a grid and the determining the propagation between the center points of each square. Each square of the grid is called a *floor-tile*. Outdoors and indoors are discretized in this manner. Indoors, each floor of the building is discretized into set of floor-tiles. To reduce the number of floor-tiles, the entire space is not discretized. Rather, floor-tiles are placed only along the centerlines of sidewalks, hallways, and roads. For rooms, floor-tiles are placed in every location that a mobile node can be present. The walls of buildings are also divided into *wall-tiles*. Since the beam tracing is in 2-D, the wall-tiles are segments (1-D tiles).

The computation is divided into two parts, preprocessing and beam tracing. During preprocessing, *ray neighbors* for each tile are found. A tile's ray neighbors are all the tiles that could be directly reached (i.e., without reflection, transmission through a wall, or diffraction) by a ray emanating from the tile. Once the ray neighbors are found, beam tracing can be performed efficiently. Figure 3 illustrates how the beam tracing computation is performed

This process of beam tracing as shown in Figure 3 is carried out in a breadth first manner with each beam continued to be reflected, transmitted, and, perhaps, subdivided until either the beam exits the modeled area or until the estimated path loss of the beam surpasses a threshold. The trade-off between the number of reflection/transmissions/diffractions and accuracy and computational complexity is investigated in the next section.

Beam tracing can be performed indoors as well as outdoors. However, the computational complexity depends on the number of walls. Since building interiors have a large number of walls, beam tracing inside all the buildings within a large region of a city exceeds today's computational abilities. Fortunately, it has been found that a realistic estimate of indoor propagation can be performed without using beam tracing. Specifically, the *attenuation factor* (AF) model has been shown to provide realistic path loss estimates, with the error found to be within 4dB [39]. The AF model assumes that communication indoors takes a straight line path (i.e., no reflections off of interior walls). Furthermore, transmissions through each interior wall and transmissions through each floor result in attenuation. While the

No	Loss (dB)
1	30
2	35
3	39
>= 4	40

Figure 4. Number of floors the signal propagates vs loss in dB [39]

amount of attenuation depends on the building, a value of 4dB per wall (for an office building) has been shown to work well [39] (also see Section 5.3). Realistic attenuation for the signal propagating through floors is given in the Table 4. In summary, outdoors, rays make reflections off of buildings, diffractions over and around buildings, and transmissions into buildings. Once inside a building, the ray will continue in the same direction, experiencing further attenuation for any interior wall or floor that it passes through. When a ray strikes an exterior wall from the inside, it is both reflected back inside and transmitted outside in the same way as rays hitting the exterior wall from the outside.

5.1 Computational complexity

Beam tracing is a feasible but highly computationally complex task. The complexity is both in terms of memory usage and processing time. Processing times for a 1km$\times$1km urban region is often on the order of tens of processor days. But the process is highly parallelizable and nearly scales with the number of processors used (i.e., 75 processor days takes about 5 days on 15 processors). Of course, the entire path loss matrix for each city only needs to be found once (several are currently available for download). Table 5 outlines the memory requirements and the processing time for two cities. These two cities represent two ends of the spectrum. Paddington is a dense city with relatively small buildings, whereas the campus has much more open space and larger buildings. Note that the campus map is significantly larger than Paddington, but only has few more buildings.

The memory requirement is dominated by the lists of ray neighbors. In Table 5, the wall-tiles were 2 meters long and floor-tiles were 1m$\times$1m. While the number of wall and floor tiles scales linearly with the reciprocal of the size of the tiles (i.e., if the wall-tiles are twice as long, there are half as many)[3], the total ray neighbors scale quadratically. For the simulations shown in Table 5, there are between 20,000 and 40,000 exterior floor-tiles, and 80,000 to 100,000 interior floor-tiles. As expected, sidewalks and roads utilize little area outdoors, but indoors, hallways and offices fill large areas. In Table 5, the floor-tiles along sidewalks and hallways were space 1 meter apart, floor-tiles along roads were spaced 2 meters apart, each office had one floor-tile, and wall-tiles were 2 meters long.

As shown in Table 5, there are on the order of 10 to 100 million ray neighbors for a city of size about 1km$\times$1km. Since each list entry has a size of 40B, the memory required approaches 4GB. Assuming sufficient memory resources, the computation time for the preprocessing stage is relatively short; the cities shown in Table 5 took a single day on an AMD Athlon 64 FX 55 with 8GB RAM.

Once the ray neighbors are found, the propagation characteristics between each pair of floor-tiles can be found. From a single source, the propagation characteristics to all destinations can be found at the same time. That is, as the beam is reflected, the illumination of any floor-tile is recorded. Table 5 shows that each source produces vertical planes that make approximately 100,000 reflections, diffractions, or transmissions. These reflections, diffractions, or transmissions are shared among all destinations. However, for each destination, all the vertical plane paths between the source floor-tile and destination floor-tile are found. Hence, the total number of vertical plane paths greatly exceeds the total number of reflections, diffractions, and transmissions.

For each source it is necessary to find all the reflections. Thus, in the campus map, the total number of reflections found was around 263 billion and 12 billion for Paddington. Several optimizations and tricks to efficiently distributed the program result in the total processing time as shown.

5.2 Impact of reflections, diffraction, and transmissions

It is of interest to determine how many reflections, diffractions, and transmissions must be modeled before the quality of the model is affected. In order to investigate the impact of the different factors, we consider propagation in Paddington, London. Table 6 shows the average of several experiments. In each experiment, the source was placed along a major street. The center column of Table 6 shows the number of locations where the signal strength was found to be sufficiently strong for communication. In this case, each location is on a sidewalk and with 1 meter between locations. The right-hand column shows the computation time in seconds. Each row corresponds to an experiment with different number of iterations, where each iteration includes a reflection, transmission, or diffraction. In some cases, the possibility of diffraction was neglected. It is clear that considering LOS greatly reduces the coverage. In this case we find the coverage found with only LOS

[3] Recall that floor tiles cover linear sidewalks.

City	Size (km
Paddington	857x836
Campus	1768 x15

Figure 5. Computational Complexity

is reduced by factor of 4.5 from the coverage achieved with all iterations. It can also be seen that diffraction must also be included; for a particular number of iterations, neglecting diffraction results in a 30%-50% reduction in coverage. In this case, after 4 iterations, the coverage reaches its maximum, both with and without diffraction. However, the beam tracing continued until 15 iterations. From a computational point of view, we see that including diffraction increases the computation by about 5%-25% and each iteration adds roughly 10%-20%. In this case there is little gain in coverage or accuracy by allowing the number of iteration to increase beyond 4. However, the computation time greatly increased. On the other hand, it is difficult to know a priori as to how many iterations are enough.

While not shown here, a similar experiment showed the impact of ground reflections to be minimal. Specifically, there is little change in coverage if the ground reflection was excluded. The reason for this is that the canceling out effect of the ground reflection (i.e., the signal strength decays like $1/d^4$ as oppose to $1/d^2$[39]) does not occur until the distance is around 200 meters[4]. However, rays that propagate 200 meters also make several reflections. These reflections change the magnitude and phase of the signal and reduce the canceling effect.

5.3 Validation

The goal of the propagation model is not to predict the signal strength, but to merely have the signal strength behave in a realistic fashion. Nonetheless, it is useful to understand the accuracy of the propagation model. Three validation experiments were performed, two outside and one inside. In all cases, an 802.11b access point and the Berkeley Varitronics Yellowjacket wireless receiver [3] were placed on 1.5 meter tripods. The access point was placed at a fixed location and wireless receiver was moved after making 600 measurements (1 minute). Figure 7 shows a part of the campus and Figure 9 shows a street intersection in Philadelphia. In Figure 7, the buildings were 14 meters high while in Figure 9 the buildings were at least 40 meters high. In both

[4]The actual distance depends on the frequency and height of the antenna. In the case of 2.4GHz and 1.5 meters heights, the distance is 200 meters.

Experiment	Coverage	Time
Line of sight	937	56
1 iter	2623	59
1 iter no diffraction	1960	56
2 iter	3927	61.5
2 iter no diffraction	2616	57
3 iter	4243	67
3 iter no diffraction	2862	58
4 iter	4265	85
4 iter no diffraction	3065	63
All iter	4265	122

Figure 6.

cases, the X-mark denotes the location of the transmitter while the receiver is moved along the indicated path. Figure 8 shows the observed and modeled path loss corresponding to the path starting from the transmission point and moving along the path in the counter-clockwise direction. Figure 10 shows the model and observed path loss starting at the transmitter, move to the right and then turning the corner.

Figures 8 and 10 show that the model and observations match well both qualitatively and quantitatively (within 5dB in most areas). To gain more insight into propagation modeling we examine the propagation prediction quality at different locations, especially the location where the prediction quality is lower. In the area marked C, there is an unmodeled archway that is depicted in Figure 7 between B and C. Similarly at location F, there is a bridge as depicted with the indicated rectangle. Ignoring these objects impacts the accuracy of the propagation prediction. In the locations marked E and G, there are several moderate sized unmodeled objects (large air conditioners at E and trees at G) that partially blocked the signal. Sometimes such small objects are called scatterers. We see that scatters can slightly decrease the received signal strength. On the other hand, in the areas where there is purely line-of-sight (marked As), line-of-sight with reflections (marked Bs) and reflections with

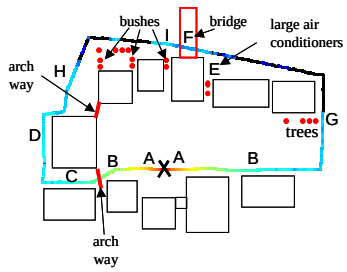

Figure 7. Campus Map.

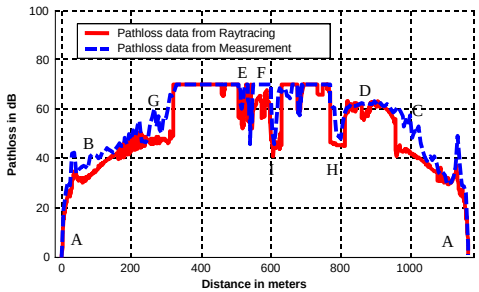

Figure 8. Observed and Predicted Path Loss in the Campus.

diffraction (marked D), there is very good agreement between the model and the observations.

Figure 10 also shows a good fit. Again, the influence of scatters can be observed. In this case the scatterers includes things such as mailboxes, parked cars, and irregularity of the walls (e.g., doors that are set back from the wall). Nonetheless, the model and observations are within a few dB.

Finally, Figure 11 shows the layout of a building interior and Figure 12 compares the modeled and observed signal strength for the points indicated in Figure 11. Again, we see that there is reasonable good agreement between the model and the observations.

In summary, it is clear that accurate propagation prediction requires more detailed knowledge of the environment. However, coarse knowledge (e.g., location of buildings alone) provides realistic propagation, both qualitatively and quantitatively.

6 Modeling Node Mobility

The performance of MANETs is clearly impact by the distribution of nodes. The majority of mobility simulators for MANETs assume that the nodes are uniformly spread or at least distributed according to a smooth distribution.

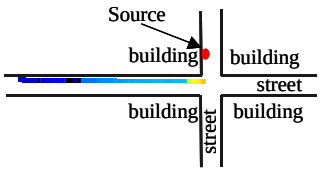

Figure 9. Intersection Map.

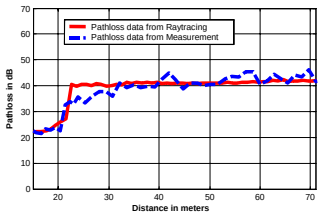

Figure 10. Observed and Predicted Path Loss at an Intersection.

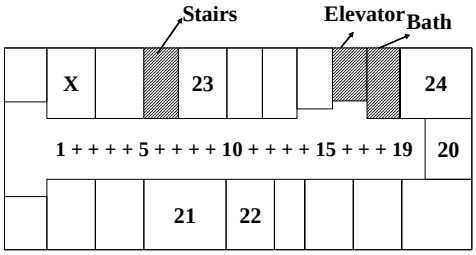

Figure 11. Interior Building Layout.

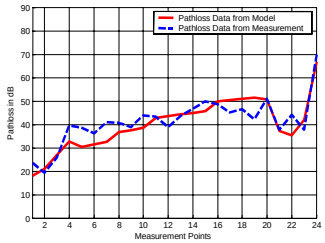

Figure 12. Interior Path Loss. The measurement points shown on the x-axis correspond to the numbered locations in Figure 11.

For example, the popular random way-point mobility model leads to a smooth distribution where nodes tend to be at the center of the modeled area [27]. Such distributions differ significantly from those that arise in realistic mobility in two ways. First, nodes are restricted to sidewalks, buildings, or roads, and second, the positions of nodes are correlated, specifically, nodes often move in groups (i.e., node arrivals are bursty). Such groups of nodes are called platoons and are well known to have an impact on the capacity of roads and sidewalks [46]. Platoons of vehicles and pedestrians can arise from traffic lights and from faster nodes catching-up, but not passing slower nodes. In the case of pedestrians, the second cause is increased by nodes that are in groups by choice. Such groups move slower than solitary nodes and limit the ability of faster nodes to pass, thus expanding the size of the group.

In this section realistic mobility modeling that accounts for these characteristics is discussed. While these models appeal to common sense, nearly all models are based on the data and experiences of urban planning and traffic engineering research communities. When available, the model parameters are derived from observations found in the literature. There are two aspects to the mobility, dynamics and node interaction, and trip generation. The dynamics and node interaction includes speed distribution, inter-node distance-speed relationship, and lane changing. As is suggested by the highway capacity manual [46], the dynamics of pedestrians and vehicles are closely related and hence can be treated almost simultaneously.

6.1 Node Dynamics and Interactions

6.1.1 Inter-node distance-speed relationship

When a node with a higher desired speed catches up with a slower moving node, it will either follow or pass. To understand the dynamics of catching up, it is necessary to understand the distance-speed relationship. The impact of this relationship is that nodes can and will be tightly packed (i.e. high density) if their speed is low (congestion), but if the speed is higher, then the nodes must be further apart (low density). Since the density of nodes plays an important role in MANET performance, the distance-speed relationship must be understood and realistically modeled. For vehicles, the distance-speed relationship, which we denote as $D(S)$, is closely related to the "two-second rule" that specifies that a following vehicle should not be closer than two seconds behind the vehicle it follows. For both vehicles and pedestrians, these relationships have been extensively studied.

In the case of vehicles, the distance-speed relationship depends on weather conditions (e.g., dry vs. wet road), on the traffic regime, and the recent traffic regime history [44], [7]. While factors such as recent traffic regime history are important in highway traffic, we only focus on the more simple urban street traffic and use the speed-distance relationships observed at low speeds where such factors are less noticeable [7]. While $D(S)$ is not exactly linear, it is often modeled as linear, specifically, $D(S) = \alpha + \beta S$. In [44], (α, β) were found to be $(1.78, 10.0)$ and $(1.45, 7.8)$ in dry conditions and $(0.415, 8.3)$ and $(0.230, 6.0)$ in wet conditions. Here, and throughout the next sections distances are in meters and speeds are in meters/sec. These values of α and β are in agreement with the observations presented in [7] and [37].

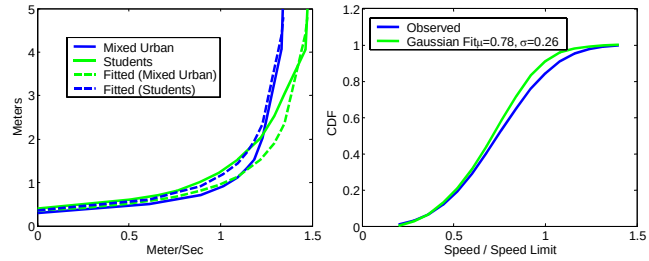

Figure 13. Left: Distance-Speed Relationship for Pedestrians. The mixed urban pedestrian data is adapted from [32] and the student observations are adapted from [28]. Right: CDF of the ratio of observed speeds to speed limit and the CDF of a fitted Gaussian distribution.

The distance-speed relationship for pedestrian is studied in [32] and [28]. Figure 13 shows the distance-speed relationship derived from these observations[5]. We approximate this relationship with $D(S) = S^* \times D_{\min} / (1.08 \times S^* - S)$ where $D_{\min}$ is the minimum distance between people without touching and S^* is the desired speed of the pedestrian. $D_{\min}$ was found to be at least 0.35m [38].

It has been found that pedestrian desired speeds are approximately Gaussian with mean 1.34 m/s and standard deviation 0.26 [15], [14], [45]. For vehicles, the ratio of the vehicle's speed to the speed limit presented in [9] can be modeled as Gaussian with mean 0.78 and standard deviation 0.26 (see Figure 13).

6.2 Lane Changing

While traffic lights are an important cause of platooning, lane changing also plays an important role [38]. A node will certainly not pass if there is no room (e.g., if the other lanes are full). Even if there is room, both pedestrian and

[5]The plot shown is based on area-speed relationships with the assumption of 0.75 meter of lateral space between people as found by Oeding [31].

vehicle nodes might not pass out of choice and select to slow down and follow the node ahead [49]. Such decisions lead to platooning.

Lane changes are grouped into two categories, discretionary and mandatory. The latter category results when the node's current lane ends or is blocked by a fixed obstruction, or the route to the destination requires changing lanes (e.g., to exit or make a turn). For MANET simulation, the dynamics of mandatory lane changes can be ignored since the exact moment when the node does change lanes will not have a significant impact of the distribution of nodes and will only have a minor impact on position (and hence a minor impact on signal propagation to and form the node).

Since discretionary lane changing is related to platooning, it must be included in MANET mobility simulation. Discretionary lane changing depends on the difference between the speed that results from not changing lanes and the speed that could be achieved if a lane was changed as well as on other factors such as the presence of large vehicles [1]. We focus only on the speed aspects of discretionary lane changing.

In [1], the probability of changing lanes was modeled as

$$P\,(\text{desire to change lanes}) = 1/\left(1 + \exp\left(A + B \times (V_* - V^*)\right)\right)$$

where V_* is the speed that the node would achieve if it remains in the current lane and V^* is the speed that would be achieved if the node changes lanes. Since speeds may experience short-term variation, instantaneous determinations of V_* and V^* leads to erratic behavior. Instead, letting ν denote the node that is considering changing lanes, we define V_* to be the average speed of all nodes between ν and the next intersection, and V^* to be the minimum of the desired speed of ν and the average speed of the nodes in the target lane that would be between ν and the next intersection.

According to the findings of [1], if a node catches up to another node and there is room, it will change lanes 50% of the time when the speed difference is $V_* - V^*$ is zero. Furthermore, when the speed difference reaches one standard deviation of the nodes speed distribution and there is room, the node will change lanes 66% of the time. To mimic this behavior at the slower speeds of urban vehicles and pedestrians, we set $A_{Vehicle} = -0.225$, $B_{Vehicle} = 0.1$, $A_{Pedestrian} = -0.225$, and $B_{Pedestrian} = 1.7$. While the Highway Capacity Manual suggests that pedestrian mobility is similar to vehicle mobility, it is not clear that the same model for making passing decisions can be used (albeit with scaled parameters). We examine the impact of these parameters in Section 6.4 and find that they do result in platooning that has been observed.

Other dynamics of lane changing include the selection of an acceptable gap between cars to change lanes into. It is not clear what the benefit of precise dynamics of gap acceptance would impact MANET simulation. Hence, we simply allow nodes to change lanes if changing lanes would not greatly disrupt the nodes in the target lane.

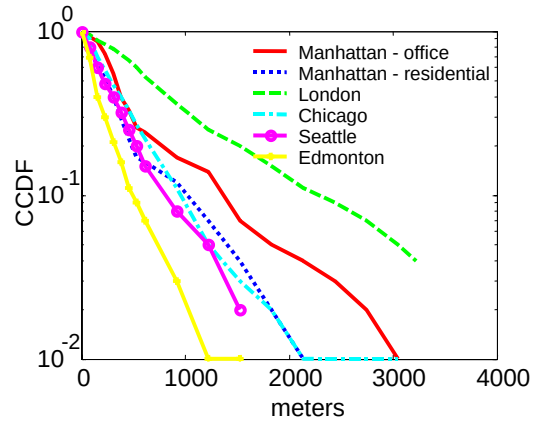

Figure 14. CCDF of Distance Traveled During Outdoor Walking Trips. This data is from [38].

Since sidewalks are bidirectional, pedestrians may change into left-hand lanes and block on-coming pedestrians. Thus, we force all pedestrians that are in left-hand lanes to immediately change to a right-hand lane when confronted with an on-coming pedestrian. Furthermore, a pedestrian does not change into a left-hand lane *[although] ; unless* there are no on-coming pedestrians from the pedestrian's position to the next intersection.

6.3 Trip generation and arrival rates

Some aspects of trip generation have been well studied. For example, many local governments require predictions of trips that will be generated by proposed residential or business developments. Transportation simulators such as TRANSIM utilize this information as well as US census data to estimate transportation demand of different members of each household. There seems to be no limit on the level of detail that could be included in trip generation. However, in order to reduce the complexity of use, a simpler approach is taken for simulation of urban MANETs. We focus on pedestrian and vehicle nodes separately.

6.3.1 Pedestrian trips

It is assumed that each building is composed of offices and each pedestrian has a home office. The pedestrian node initiates trips from its office at random times. In some cases, the node remains within the building while in other cases it leaves the building. The rate at which nodes enter and leave buildings has been well studied with extensive data provided in [38] (especially tables 2.5, 2.8 and Figures 2.1

and 2.2). It has been found that for office buildings, occupants make an average of 2.3 to 4.7 in or out trips per twelve-hour day. This amounts to a mean time between entering and exiting the building between 2.3 and 5.3 hours. In the case of restaurants, supermarkets, department stores and residences, the average time to remain in the building is 3.75, 0.6, 1.25, 5.2 hours respectively. However, in most cases, the duration is not uniform. During the lunch hours, office occupants' time to next departure is between 2 and 6 times less than the mean (i.e., between 0.38 and 2.65 hours)[6]. During non-lunch hours and during the non-rush hours, the mean duration in the building drops to values between the average and double the average duration in the building. Similar values are found for other establishments with restaurants achieving a mean duration of 3 times less than average or 1.15 hours. Thus, while the duration a node remains in a building before exiting depends on the time of day, the building, and the establishment, durations range from around 25 minutes to 6 hours. Since lunchtime is rather nonstationary, afternoon rates might be preferable which range from 1.25 hours for department stores to 5 hours for offices. We denote the mean time between trips that leave the building as m.

Unfortunately, there is much less data on the trips people take within buildings. Without such data we are forced to make a guess based on our own experiences. We selected to model the duration between trips as exponentially distributed with mean μ where $\mu \leq m$. Thus, the fraction of trips that lead the node outside is μ/m. Hence durations within the building are also exponentially distributed.

Groups of pedestrians play an important role in platooning [38]. Again, there is little data on the frequency of groups. However, we have made observations of over 500 pedestrians in an urban street and found the number of pedestrians within a group is well modeled with the Zipf distribution with shape parameter of 2.18, i.e., $P\left(\text{Group size} \geq g\right) = 1/g^{2.18}$. We allow groups of node to congregate in an office and then proceed to a destination. While in transit, the nodes walk abreast of each other unless there are on-coming nodes or when the sidewalk can support all the nodes in the group. In such cases, some nodes will follow behind. The speed of the group members is forced to be the same and the nodes cross intersections with the grouping intact. The dynamics of groups acts to block other nodes from passing as observed by [38].

For outdoor trips, the duration and distance traveled has been well observed (e.g., see [38]). Figure 14 shows the complementary cumulative distribution (CCDF) of the distance traveled during walking trips in different cities. The distribution is well modeled by an exponential distribution with means 554m, 380m, 403m, 344m, 813m, and 216m for Manhattan from office buildings, Manhattan from residences, Chicago, Seattle, London and Edmondton respectively. We see that the US cities have approximately the same mean. Thus, once a node selects to travel outside, it then selects a range of distances to travel. Buildings within that range are selected uniformly and offices with the selected building are also selected uniformly.

[6] A maximum of 2.65 hours in the building before the next trip does not agree with a mean number of 2.3 trips per day. However, the rate of 2.65 is only for the lunch hour. Nodes that do not leave during this period of high exit rate are subject to the longer duration inside the building that occurs after the lunch.

6.3.2 Vehicle trips

Traffic simulators such as CORSIM [10] allow vehicle trips to be generated in two ways, with origin-destination (O-D) flow matrices or with turning probabilities. With O-D matrices, the rate at which vehicles enter the simulated region at a origin O and proceed to the destination D is given by the O, D element of the O-D matrix. If only turning probabilities are used, vehicles enter into the modeled area at one of the preselected locations and proceed until the vehicle arrives at any exit location (often at the edge of the modeled area). At each intersection, vehicles turn or go straight according to the turning probabilities assigned to that intersection. O-D matrices yield a more accurate simulation, however, accurate O-D matrix are difficult to determine, whereas turning probabilities can be determined by simply counting vehicles turning at each intersection. Thus, both approaches are used for urban traffic engineering.

Drawbacks of turning probabilities are that vehicles might travel in long loops or meander through the city for extended periods of time. However, since turning probabilities are quite small (often they are in the range of 0.3 to 0.1 [16]) such unrealistic behavior is rare; most trips proceed through the city with only a few turns. Our simulator currently uses homogeneous turning probabilities. Exit and entry points are defined by the map as described in Section 4.

To model the rate that vehicles enter the city, we borrow urban traffic models for "upstream" lights (i.e., the traffic that exits a light upstream of the light under investigation). The upstream traffic is from two sources, vehicles that pass through the green light and go straight, and vehicles that turn on to the street. Following [22], it is sufficient to assume that the number of vehicles that enter is Poisson with mean

$$\frac{\lambda_{VehicleStartRate} \times \text{Signal Period} \times (1 - prob_turning)}{\text{Number of Entering Roads}}$$

conditioned on that the number does not exceed the number that can pass through an intersection during a single green light. These vehicles enter at periodic moments with period equal to the traffic signal period. Furthermore, the number of turning vehicles into the road that leads to the modeled

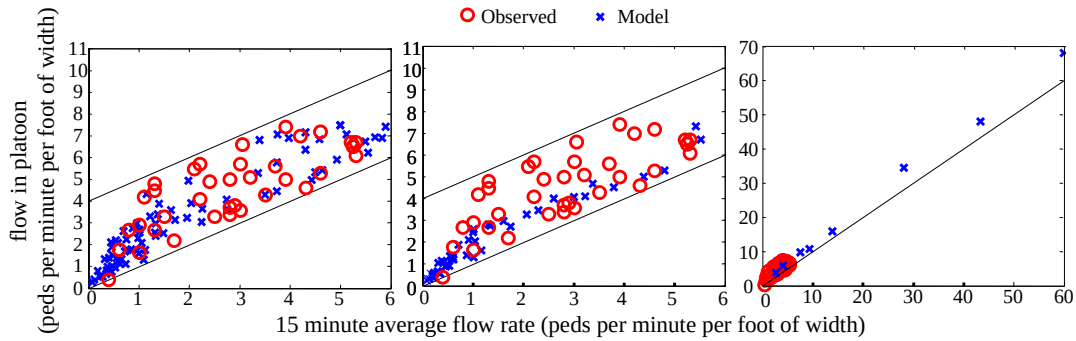

Figure 15. 15 Minute Average Flow Rate versus Flow Rate in a Platoon. The flow rate is the number of pedestrians that pass by the measurement point per minute divided by the width (in feet) of the sidewalk. The black line is the area of realistic values found by Pushkarev and Zupan.

area is Poisson process, but with rate

$$\frac{\lambda_{VehicleStartRate} \times prob_turning}{\text{Number of Entering Roads}}.$$

Hence, the total average rate that vehicles enter the city is $\lambda_{VehicleStartRate}$.

6.4 Validation of Pedestrian Mobility

The burstiness of pedestrians, or in the terminology of traffic engineering, pedestrian platoons, have been investigated by Pushkarev and Zupan [38]. Their work has served as the basis for the pedestrian traffic engineering guidelines set forth in the Highway Capacity Manual [46]. The metrics of burstiness for pedestrian platoons are different from the ones typically used in studying data networks. Specifically, Pushkarev and Zupan compare two flow metrics, the 15 minute average flow rate (AFR) and the flow rate during a platoon (PFR). A node is in a platoon if the local density of nodes exceeds the average density. As is shown in the Figure 15, the PFR is higher than the AFR. According to Pushkarev and Zupan, the larger the PFR compared to the AFR, more bursty the pedestrian traffic is. The study of Pushkarev and Zupan was not focused on finding the frequency of specific flow rates, but to examine what combinations of AFR and PFR occur on urban sidewalks. Thus, we use this data as a baseline with which we compare the pedestrian mobility model described above. The left-hand plot in Figure 15 shows two sets of data. The generated data from the mobility model is from a variety of configurations including counting pedestrians on a block with and without buildings, various sizes of sidewalks (from 4 lanes to 32 lanes), various traffic light timings (from 60 seconds to 120 second periods), and various rates of pedestrians flowing into the street.

As can be seen from the left-hand plot in Figure 15, the mobility model described above generates combinations of PFR and AFR that are realistic. The center plot in Figure 15 shows the data set collected by Pushkarev and Zupan and a set of data generated by the mobility model but where nodes pass whenever there is room to pass, i.e., P (desire to change lanes) $= 1$ as opposed to what is given in [1]. Clearly, increasing the propensity to change lanes acts to decrease the burstiness so that some realistic levels of burstiness never occur. Finally, the right-hand plot in Figure 15 shows Pushkarev and Zupan's data compared to data generated by the mobility model but where there are no inter-pedestrians dynamics, i.e., nodes move along lane irrespective of other nodes. Such mobility allows, for example, nodes to exceed the distance-speed relationship. As shown in Figure 15, ignoring inter-node dynamics results in unrealistic levels of congestion (according to Pushkarev and Zupan the flow rate rarely exceeds 18).

7 Conclusions

Realistic simulation techniques for mobile ad hoc networks in urban areas have been presented. These techniques include methods to realistically simulate propagation and mobility. While realistic propagation modeling is computationally expensive, the propagation matrix needs to only be computed once for each urban map. Based on the findings from urban planning and traffic engineering research community, realistic mobility models can be developed. It is evident that these models are far more realistic than the random waypoint open-space propagation models that are widely used now. One challenge in realistic simulation is to keep the usage complexity low. The methods, models, and model parameters developed in this paper reduce the complexity of use while still maintaining realistic simulation.

References

[1] K. I. Ahmed. *Modeling Drivers' Acceleration and Lane Changing Behavior*. PhD thesis, MIT, 1999.

[2] F. Bai, N. Sadagopan, and A. Helmy. Important: a framework to systematically analyze the impact of mobility on performance of routing protocols for adhoc networks. In *InfoCom*, 2003.

[3] Berkeley Varitronics. http://www.bvsystems.com/.

[4] S. Bohacek and V. Sridhara. The graph properties of MANETs in urban environments. In *Proceedings of Forty Second Annual Allerton Conference on Communication, Control, and Computing*, 2004.

[5] T. Camp, J. Boleng, and V. Davies. A survey of mobility models for ad hoc network research. *WCMC*, 2(5):483–502, 2002.

[6] S. Cass.

[7] T. Dijker, P. H. L. Bovy, and R. G. M. M. Vermijs. Car following behavior in different flow regimes. In P. H. L. Bovy, editor, *Motorway Traffic Flow Analysis*, pages 49–70. delft university press, Delft, the Netherlands, 1998.

[8] J.-M. Dricot and P. D. Doncker. High-accuracy physical layer model for wireless network simulations in NS-2. In *IWWAN*, 2004.

[9] J. Du and L. Aultman-Hall. An investigation of the distribution of driving speeds using in-vehicle GPS data. In *Vermont Institute of Transportation Engineers Annual Meeting*, 2004.

[10] FHWA. *CORSIM User's Manual, Version 5.0*. ITS Research Division, FHWA, 2000.

[11] S. Floyd and V. Paxson. Difficulties in simulating the internet. *IEEE/ACM ToN*, 9:392–403, 2001.

[12] GIS. Geographic information system. http: www.gis.com.

[13] O. Heckmann, M. Piringer, J. Schmitt, and R. Steinmetz. On realistic network topologies for simulation. In *Proceedings of the ACM SIGCOMM Workshop on Models, Methods and Tools for Reproducible Network Research*, 2003.

[14] D. Helbing. The statistics of crowd fluids. *Nature*, 229:381, 1971.

[15] D. Helbing. Sexual differences in human crowd motion. *Nature*, 240:252, 1972.

[16] J. E. Hummer. Unconventional left-turn alternatives for urban and suburban arterials. *ITE Journal*, 68, 1998.

[17] A. Jardosh, E. M. Belding-Royer, K. C. Almeroth, and S. Suri. Towards realistic mobility models for mobile ad hoc networks. In *MobiCom*, 2003.

[18] P. Johansson, T. Larsson, N. Hedman, B. Mielczarek, and M. Degermark. Scenario-based performance analysis of routing protocols for mobile ad-hoc networks. In *MobiCom*, 1999.

[19] D. Johnson and D. Maltz. Dynamic source routing in ad hoc wireless networks. In Imielinski and Korth, editors, *Mobile Computing*, pages 153–181. kluwer academic publishers, 1996.

[20] E. C. Jordan and K. G. Balmain. *Electronmagnetic Wave and Radiating Systems*. Prentice hall, NJ, 1968.

[21] J. Kaba and D. Raichle. Testbed on a desktop: Novel testbed strategies for multi-hop MANET routing protocol development. In *Mobihoc*, 2001.

[22] A. Kamarajugadda and B. Park. Stochastic traffic signal timing optimization. Technical Report UVACTS-15-0-44, Center for transportation studies at the university of Virginia, 2003.

[23] A. Konrad, B. Y. Zhao, A. D. Joseph, and R. Ludwig. A markov-based channel model algorithm for wireless networks. In *MSWiM*, 2001.

[24] L. Li, D. Alderson, W. Willinger, and J. Doyle. A first-principles approach to understanding the internet's router-level topology. In *SIGCOMM*, 2004.

[25] Y. Liu, F. L. Presti, V. Misra, D. Towsley, and Y. Gu. Fluid models and solutions for large-scale IP networks. In *SIGMETRICS*, 2003.

[26] D. A. McNamara, C. W. Pistorius, and J. A. G. Malherbee. *Introduction to Uniform Geometrical Theory of Diffraction*. Artech House, 1990.

[27] W. Navidi and T. Camp. Stationary distributions for the random waypoint mobility model. *IEEE transactions on Mobile Computing*, 3:99–108, 2004.

[28] F. P. D. Navin and R. J. Wheeler. Pedestrian flow characteristics. *traffic engineering*, pages 30–36, 1969.

[29] Network Simulator - NS-2. http://www.isi.edu/nsnam/ns/.

[30] Network Simulator - NS-2. Wireless and mobility extensions to ns-2 http://www.monarch.cs.cmu.edu/cmu-ns.html.

[31] D. Oeding. Traffic loads and dimensions of walkways and other pedestrian circulation facilities. *Strassenbau and strassenverkehrstechnik*, 22, 1963.

[32] S. J. Older. Movement of pedestrian on footways in shopping street. *traffic engineering and control*, pages 160–163, 1968.

[33] OPNET. http://www.opnet.com.

[34] F. H. P., Fitzek, L. Badia, P. Seeling, J. G. Schulte, and T. Henderson. Mobility and stability evaluation in wireless multi-hop networks using multiplayer games. In *Proceedings of NetGames*, 2003.

[35] Y. I. H. Parish and P. Müller. Procedural modeling of cities. In *Proceedings of the 28th Annual Conference on Computer Graphics and Interactive Techniques*, 2001.

[36] Philadelphia Mayor's Office. Government leaders teleconference - wireless: The 21stCentury techhology http://www.phila.gov/mois/press/multimedia/pdfs/wirelessphiladelphia092004.pdf, 2004.

[37] J. Piao and M. McDonald˙ Analysis of stop and go driving behavior through a floating vehicle approach. In *Proc. Of the IEEE Intelligent Vehicles Symposium*, 2003.

[38] B. Pushkarev and J. M. Zupan. *Urban Space for Pedestrians*. MIT press, 1975.

[39] T. Rappaport. *Wireless Communications - Principles and Practice*. Prentice Hall, 2002.

[40] K. Rizk. *Propagation in Microcellular and Small Cell Urban Environment*. PhD thesis, Swiss Federal Institute of Technology of Lausanne, 1997.

[41] K. Rizk, R. Valenzuela, S. Fortune, D. Chizhik, , and F. Gardiol. Lateral, full-3d and vertical plane propagation in microcells and small cells. In *Proceedings of the IEEE 48th Vehicular Technology Conference*, 1998.

[42] Scalable Network Technologies. The QualNet simulator http://www.qualnet.com/.

[43] R. Schwendener. Indoor radio channel model for protocol evaluation of wireless personal area networks. In *PIMRC*, 2002.

[44] S. Shekleton. A GPS study of car following theory. In *Conference of Australian Institutes of Transport Research (CAITR)*, 2002.

[45] G. K. Still. *Crowd Dynamics*. PhD thesis, university of warwick, 2000.

[46] Transportation Research Board. *2000 Highway Capacity Manual*. National Research Council, Washington, D.C., 2000.

[47] WaveCall. WaveSight http://www.wavecall.com/.

[48] WirelessValley. LANPlanner http://www.wirelessvalley.com.

[49] Y. Zhang, L. E. Owen, and J. E. Clark. A multi-regime approach for microscopic traffic simulation. In *The 77th TRB Annual Meeting*, 1998.